AIP | The Journal of Chemical Physics

Finite-temperature quantum simulations of mixed rare gas clusters

Markus Meuwly and J. D. Doll

Citation: The Journal of Chemical Physics **132**, 234315 (2010); doi: 10.1063/1.3431080
View online: http://dx.doi.org/10.1063/1.3431080
View Table of Contents: http://scitation.aip.org/content/aip/journal/jcp/132/23?ver=pdfcov
Published by the AIP Publishing

Finite-temperature quantum simulations of mixed rare gas clusters

Markus Meuwly[1,2,a)] and J. D. Doll[2,b)]
[1]*Department of Chemistry, University of Basel, Klingelbergstrasse 80, CH-4056 Basel, Switzerland*
[2]*Department of Chemistry, Brown University, Providence, Rhode Island 02912, USA*

(Received 1 March 2010; accepted 28 April 2010; published online 21 June 2010)

Finite-temperature quantum Monte Carlo simulations are presented for mixed neon/argon rare gas clusters containing up to $n=10$ atoms. For the smallest clusters ($n=3$) comparison with rigorous bound state calculations and experiments shows that the present approach is accurate to within fractions of wavenumbers for energies and to within a few percent or better for rotational constants. For larger cluster sizes, for which no rigorous quantum calculations are available, comparison with experiment becomes even more favorable. In all simulations accurate pair potentials for the rare gas-rare gas interactions are employed and comparison with high-level electronic structure calculations suggest that many-body interactions play a minor role. For the largest clusters investigated (Ne_4Ar_6) gradual melting of the neon phase is observed while the argon-phase remains structurally intact. © *2010 American Institute of Physics*. [doi:10.1063/1.3431080]

I. INTRODUCTION

Clusters, understood as weakly interacting aggregates of individual particles, exhibit unique properties from structural and dynamical perspectives. A model for such compounds are pure or mixed rare gas clusters, which have attracted considerable attention both experimentally and theoretically. Of particular interest is the opportunity to study the relationship between structure and dynamics as a function of the size and composition of such clusters. Furthermore, many details of intermolecular interactions and the influence of quantum effects can be investigated at a level of detail that is otherwise not accessible.

High resolution spectroscopy of rare gas dimers, trimers, and tetramers has established that even small aggregates of rare gases can be sufficiently stabilized in supersonic jets to allow analysis of their rotational spectra.[1,2] Comparison with calculated spectra from quantum bound state calculations using pairwise-additive potentials and those including nonadditive corrections suggested that the pairwise potentials may require adjustments.[3] The necessary corrections appeared larger for Kr- and Xe-containing systems but relatively small for Ar-containing clusters. More recently, melting temperatures for neon and argon clusters containing up to $N=923$ atoms have been determined[4,5] using a range of potential energy functions, including conventional and extended Lennard-Jones potentials, interaction potentials including three-body terms, and potentials derived from experimental data.[6,7] The latter have been determined from fits to a range of experimental and theoretical data, including measured second virial coefficients, transport properties, spectroscopic data, and calculated C_6, C_8, and C_{10} coefficients. The Monte Carlo (MC) simulations with different potentials showed that using accurate representations of the intermolecular interactions provides melting temperatures T_m for $N\rightarrow\infty$ in close agreement with bulk measurements, whereas T_m from simulations with conventional Lennard-Jones potentials were too low compared to experiment.[4,5] Also accurate interaction potentials and Lennard-Jones potentials have been used to investigate and compare the minimum energy structures of argon clusters up to Ar_{55}.[8] Here, the only difference found was for the structure of Ar_{21}. Thus, depending on the property of interest the quality of the interaction potential did or did not appreciably affect the computed results.

In the present work we use quantum simulations together with accurate interaction potentials[6,7,9] to characterize the spectroscopic properties of experimentally investigated mixed rare gas dimers, trimers, and tetramers and make predictions for pentamers and selected larger NeAr clusters. Of particular interest are structural properties and stabilities of the systems as a function of temperature and the expected magnitude of many-body interactions. The method of choice for such investigations are path integral calculations as they allow to include quantum effects at finite temperature.

II. COMPUTATIONAL METHODS

A. Intermolecular interaction potentials

The interactions between rare gas atoms have been extensively studied. Using experimental data from molecular beam scattering, gas imperfections and transport properties functional forms of varied sophistication have been fitted to reproduce the observations. In the present study we employ the following pair potentials: The Ne–Ne interaction is represented by the HFD-B potential of Aziz and Slaman,[6] for Ar–Ar the HFDID1 potential of Aziz[7] is used, and for Ne–Ar the HFD-B model of Barrow and Aziz[9] is employed.

In all cases experimental data ranging from viscosity measurements to high-resolution ultraviolet spectroscopy or low-energy total cross section measurements were used to fit the parameters of the model potential. The potentials reproduce various microscopic and macroscopic properties. This

a)Author to whom correspondence should be addressed. Electronic mail: m.meuwly@unibas.ch.
b)Electronic mail: jimmie_doll@brown.edu.

is advantageous for the present purposes because the main interest is in following the evolution of the absorption spectra over a range of cluster sizes. In the present work no additional terms to account for many-body interactions are retained although some work in this respect exists.[3] To increase computational efficiency, the interactions and their derivatives with respect to r required for gradient partial averaging (GPI) (see below) have been stored in lookup tables with a grid spacing of $0.02a_0$.

B. Fourier path integral simulations

In the present work the Fourier path integral Monte Carlo (FPIMC) with GPA is used to sample the equilibrium density matrix $\rho = \exp^{-\beta H}$, where $\beta = 1/(k_B T)$, k_B is the Boltzmann constant, T is the temperature, and H is the Hamilton operator of the system. There are a number of specialized reports on FPI, its variants, and comparisons with discretized FPI methods. Therefore, only a brief summary of FPI-GPA and the methods employed to treat mixed clusters is presented here.

In the position representation the density matrix can be written as

$$\rho(x,x';\beta) = \langle x'|\exp^{-\beta H}|x\rangle = \int Dx(\tau)\exp^{-S[x(\tau)]}, \tag{1}$$

where $S[x(\tau)]$ is the classical action integral in imaginary time τ,

$$S[x(\tau)] = \frac{1}{\hbar}\int_0^{\beta\hbar} d\tau\left[\frac{m\dot{x}^2(\tau)}{2} + V(x(\tau))\right], \tag{2}$$

and $Dx(\tau)$ represents the sum over all paths connecting x and x' in imaginary time $\beta\hbar$. In the FPI method an arbitrary path connecting x and x' is represented by a Fourier series,

$$x(\tau) = x + (x'-x)\tau/(\beta\hbar) + \sum_{k=1}^{k_{\max}} a_k \sin\frac{k\pi\tau}{\beta\hbar}. \tag{3}$$

Substituting $x(\tau)$ into the expression for the action $S[x(\tau)]$ yields

$$S(x,x',\vec{a}) = \frac{m(x'-x)^2}{2\hbar^2\beta} + \sum_{k=1}^{\infty}\frac{a_k^2}{2\sigma_k^2} + \beta\bar{V}, \tag{4}$$

with the fluctuation parameter $\sigma_k = \frac{2\beta\hbar^2}{m\pi^2k^2}$, where m is the mass of the particle and $\hbar$ is the Planck constant, and the time-averaged potential

$$\bar{V} = \frac{1}{\beta\hbar}\int_0^{\beta\hbar} d\tau V[x(\tau,\vec{a})]. \tag{5}$$

This integral is conveniently carried out using Gaussian quadrature.[10]

III. RESULTS

A. Mixed rare gas dimers and trimers

Accurate data for mixed NeAr clusters are available for Ne_2Ar and $NeAr_2$ from quantum mechanical solutions of the three-dimensional Schrödinger equation, which provided ground state energies and rotational constants.[3] In this work the Ne–Ne, Ar–Ar, and Ne–Ar potential energy functions described above and a number of slightly modified potentials were used.[6,7,9] To establish the validity of the approach taken here, total energies and rotational constants were calculated for Ne_2Ar and $NeAr_2$ using FPI-GPA. The FPI-GPA calculations were carried out for $T=1$, 2, and 5 K and for $k_{\max}=8$, 16, 64, and 128, and the results were then extrapolated to k_∞ (using a convergence proportional to $1/k^2$ as in Ref. 11) and to $T=0$ (with an $\exp^{-\alpha T}$–dependence), which yield $E_{T\to 0}^{k\to\infty}$. A total number of 5×10^6 MC configurations were averaged to calculate the final results and their fluctuations. Typically, the convergence of the ground state energy is better than $0.25\ \text{cm}^{-1}$.

TABLE I. Total energies and rotational constants from FPI simulations of the $n=3$ clusters. Extrapolations to $k\to\infty$ and $T\to 0$ are carried out as explained in the text. Comparison is made with previous bound state calculations and results from high-resolution experiments.

	E (cm^{-1})	A (MHz)	B (MHz)	C (MHz)
		Ne_2Ar		
FPI $k=128$ $T=1$ K	-83.2 ± 0.1	5034 ± 120	2418 ± 30	1617 ± 30
FPI $k=\infty$ $T=1$ K	-83.0	4971	2448	1623
FPI $k=64$ $T\to 0$ K	-85.5	4992	2452	1627
Bound state[a]	-85.523	4743.43	2480.60	1589.67
Experiment[b]		4734.1	2484.64	1597.88
		$NeAr_2$		
FPI $k=128$ $T=1$ K	-149.2 ± 0.1	3441 ± 60	1743 ± 20	1152 ± 20
FPI $k=\infty$ $T=1$ K	-149.4	3474	1743	1155
FPI $k=64$ $T\to 0$ K	-152.7	3472	1745	1156
Bound state[a]	-153.372	3399.01	1746.20	1136.12
Experiment[b]		3402.77	1739.72	1137.30

[a]Reference 3.
[b]Reference 1.

Extrapolated ground state energies $E_{T\to 0}^{k\to\infty}$ (see Table I) agree favorably with the converged basis set calculations by Ernesti and Hutson.[3] The rotational constants show deviations of up to 5%. However, in most cases the rotational constants are within 2% of the accurate basis set calculations. Rotational constants from the bound state calculations were calculated by imposing Eckart conditions.[3] Such a procedure was not employed here. For Ar–CO_2 differences between conventionally calculated rotational constants and the ones explicitly taking into account Eckart conditions differ by up to 0.5%.[12] These results show that the approach taken here is meaningful. Part of the remaining discrepancies are due to interpolation of the potential energy functions and differences between FPI-GPA and explicit basis set calculations.

Furthermore, bound state calculations and FPI-GPA simulations were carried out and compared for the NeAr dimer. With the HFD-B potential of Barrow and Aziz[9] the one-dimensional Schrödinger equation using the LEVEL computer program was solved.[13] The ground state energy and the corresponding rotational constant B were found to be $-34.067\ \text{cm}^{-1}$ and 2891.5 MHz, respectively. This compares with $-34.360\ \text{cm}^{-1}$ and 2900.1 MHz from FPI-GPA calcula-

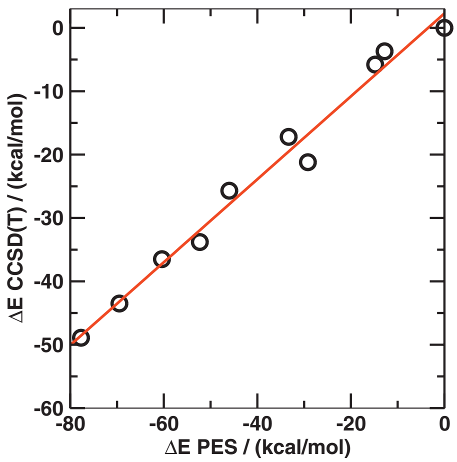

FIG. 1. Correlation of energy differences ΔE from model potentials and CCSD(T)/aug-cc-pvqz calculations. ΔE is calculated relative to the lowest energy of each method, respectively. With both methods the same structure is the one with the lowest energy.

tions with $k=128$ at 1, 2, and 5 K extrapolated to $T=0$ as done above.

Finally, to validate the empirical potential energy curves for the Ne–Ne, Ne–Ar, and Ar–Ar interactions, ten arbitrary snapshots from FPI-GPA simulations of Ne_2Ar at $T=1$ K were stored. The energies E_i of the ten structures covered a range of approximately 70 cm^{-1} in their total energies, as calculated from the empirical potentials. For all structures the total electronic energy was also calculated at the CCSD(T)/aug-cc-pVQZ level using MOLPRO.[14] In Fig. 1 energy differences $\Delta E=E^{min}-E_i$ are plotted for both the empirical potentials and the quantum chemical calculations. Here, E^{min} is the lowest of the ten energies encountered in the FPI-GPA simulations. As can be seen the correlation between energies from the empirical potentials and from highly accurate quantum chemical calculations is excellent. However, the total energies differ by up to 30 cm^{-1}, which suggests that a contribution to the total energy is missing in the pair potentials. This point is further addressed in the discussion.

B. Quantum energetics for larger mixed clusters

One of the major advantages of MC methods is that they scale more favorably with the system size than wave function-based methods to accurately solve the nuclear Schrödinger equation. Given the good agreement with converged basis set calculations for NeAr, Ne_2Ar, and $NeAr_2$, FPI-GPA calculations were also used to investigate the structure and energetics of Ne_2Ar_2, isotopically substituted $^{22}Ne_2Ar_2$, $^{20}Ne_2{}^{22}NeAr_2$, $^{20}Ne^{22}Ne_2Ar_2$, different pentamers, and Ne_6Ar_4 clusters. For the four-atom clusters spectroscopic data are available but no calculations and for the $n=5$ and $n=10$ atom clusters no detailed information is available as yet. They had, however, been investigated in previous classical dynamics simulations.[15]

The four-atom clusters were investigated in the past by using microwave spectroscopy.[1] For Ne_2Ar_2, $^{22}Ne_2Ar_2$, $^{20}Ne^{22}Ne_2Ar$, and $^{20}Ne_2{}^{22}NeAr$ total stabilization energies and average rotational constants averaged over five independent runs, each with 5×10^6 MC steps, were determined at $T=1$ K. The results are summarized in Table II. For the rotational constants absolute percentage differences between experiment and computations range from 0.1% to 1.0% whereas the absolute values of the computed rotational constants can differ by up to 100 MHz from the measured ones. It should, however, be noted that the model Hamiltonian to analyze the experimental spectra included higher centrifugal distortion constants, which affects the direct comparison of rotational constants. Comparisons for isotopically substituted clusters along the same lines and using the interaction potentials employed in the present work are available from calculations on $^{20}NeAr_2$ and $^{22}NeAr_2$.[16] They give absolute percentage differences from 0.01% to 0.05%, which is about an order of magnitude better than from FPI-GPA calculations for the four-atom clusters. The total energies for the different isotopic compositions at 1 K agree with what one would expect: Clusters containing a larger number of heavier Ne-isotopes are stabilized over those containing a smaller number of them. For the $^{22}Ne_2Ar_2$ and $^{20}Ne_2Ar_2$ the difference is 1.6 cm^{-1} whereas for $^{20}Ne^{22}Ne_2Ar$ compared to $^{20}Ne_2{}^{22}NeAr$ it is 0.9 cm^{-1}. No accurate bound state calculations for isotopically substituted NeAr trimers are available with which this can be compared. However, for $^{20}Ne_2\,{}^{82,83,86}Kr$ the cluster containing the heaviest isotope is stabilized over the two lighter ones by 0.08 and 0.1 cm^{-1}, respectively, using additive interaction potentials.[3]

TABLE II. Total energies and rotational constants from FPI simulations for selected $n=4$ clusters. Comparison is made with results from high-resolution experiments. For additional comparison between simulations and experiment, relative changes in rotational constants between clusters containing ^{20}Ne and ^{22}Ne isotopes are reported.

	E (cm^{-1})	A (MHz)	B (MHz)	C (MHz)
	$^{20}Ne_2Ar_2$			
FPI $k=128$ $T=1$ K	-237.3 ± 1.1	1779 ± 20	1247 ± 22	1053 ± 13
Experiment[a]		1771.665[a]	1261.997	1075.974
	$^{22}Ne_2Ar_2$			
FPI $k=128$ $T=1$ K	-238.9 ± 0.7	1672 ± 12	1215 ± 18	1027 ± 17
Experiment[a]		1649.468	1231.156	1051.255
Ratio $^{22}X/^{20}X$ expt.		0.931	0.976	0.977
Ratio $^{22}X/^{20}X$ simulation		0.940	0.974	0.976
Percentage difference		1.00	0.20	0.12
	$^{20}Ne_2{}^{22}NeAr$			
FPI $k=128$ $T=1$ K	-153.68 ± 0.4	2291 ± 25	1540 ± 14	1382 ± 15
Experiment[a]		2266.0	1504.342	1475.863
	$^{20}Ne\,{}^{22}Ne_2Ar$			
FPI $k=128$ $T=1$ K	-154.60 ± 0.1	2227 ± 20	1515 ± 24	1360 ± 22
Experiment[a]		2216.8	1478.694	1448.747
Ratio $^{22}X/^{20}X$ expt.		0.978	0.983	0.982
Ratio $^{22}X/^{20}X$ simulation		0.972	0.984	0.984
Percentage difference		−0.63	0.07	0.27

[a]Reference 1.

Using FPI-GPA calculations it is also possible to predict

TABLE III. Total energies and predicted rotational constants from FPI simulations for selected $n=5$ clusters. Results for species of the general form Ne_2Ar_3 and $NeAr_4$ are reported.

	E (cm^{-1})	A (MHz)	B (MHz)	C (MHz)
$^{20}Ne_2Ar_3$	-458.90 ± 0.6	897 ± 4	819 ± 6	766 ± 7
$^{22}Ne_2Ar_3$	-461.31 ± 0.6	884 ± 6	789 ± 6	736 ± 5
$^{20}NeAr_4$	-610.20 ± 0.7	862 ± 6	630 ± 4	593 ± 3
$^{22}NeAr_4$	-611.33 ± 0.6	860 ± 6	614 ± 2	578 ± 3

expected rotational constants for larger, as yet unobserved mixed rare gas clusters. Such predictions will be useful for future experiments in assisting the search for their transitions. Here, results for illustrative five- and ten-atom clusters are reported. For the five-atom clusters the $^{20}Ne_3Ar_2$, $^{22}Ne_3Ar_2$, $^{20}Ne_4Ar$, and $^{22}Ne_4Ar$ were chosen, whereas for the ten-atom cluster results for the $^{20}Ne_6Ar_4$ are discussed. In all cases averages over five independent runs each with 5×10^6 MC steps at $T=1$ K are reported.

The $n=5$ clusters provide an opportunity to scrutinize the effect of many-body interactions. Table III shows that the $^{22}Ne_3Ar_2$ cluster is stabilized by 2.41 cm^{-1} relative to $^{20}Ne_3Ar_2$, whereas the difference between $^{22}Ne_4Ar$ and $^{20}Ne_4Ar$ is only 1.12 cm^{-1}. The structures of all four clusters were optimized using MP2 calculations with a 6-311G(2d,p) and a cc-VTZ basis set and harmonic frequencies were calculated.[17] The energy differences from electronic structure calculations were 3.51 and 3.07 cm^{-1} and 1.76 and 1.31 cm^{-1}, respectively, with the smaller and larger basis sets. These numbers compare well with the data from FPI-GPA simulations. It should be noted that in the latter case fully anharmonic vibrational corrections to the total energy are included whereas electronic structure calculations only take harmonic frequencies into account.

For the larger Ne_6Ar_4 clusters the calculated rotational constants were $A=402 \pm 2$ MHz, $B=253 \pm 1$ MHz, and $C=243 \pm 2$ MHz, respectively. Radial distribution functions for different types of atom separations were calculated from simulations between 1 and 10 K (see Fig. 2). At the lowest temperatures the expected shell-like structure is observed. As the temperature increases the shells become less well defined until the features in the radial distribution functions wash out, which is indicative of considerable mixing or even melting. In particular, the Ne–Ne distance that is suggestive of a two-shell structure at 1 and 2 K looses all its structure beyond 5 K whereas the Ar–Ar distances remain around $7.5a_0$. Thus, the phase which interacts less strongly (Ne with Ne) is not able to retain its shape beyond 5 K, whereas the more strongly interacting phase maintains its internal structure. A typical structure of Ne_6Ar_4 is shown in Fig. 3.

IV. DISCUSSION AND CONCLUSIONS

The present work has established that using FPIMC methods together with accurate interaction potentials provides a deeper understanding of the structural, energetic, and spectroscopic properties of small rare gas clusters. In particular, the computations can be directly compared to experiments. It is found that rotational constants cannot be computed with the same accuracy as from wave function-based methods. This disadvantage is, however, outweighed by the fact that larger clusters can be treated. The first quantum simulations for the mixed NeAr tetramers and pentamers were carried out and the results show that rotational constants for clusters containing a different number of isotopes can be calculated with less than 1% error. In all cases such accuracy is found to be sufficient to allow assignment of the

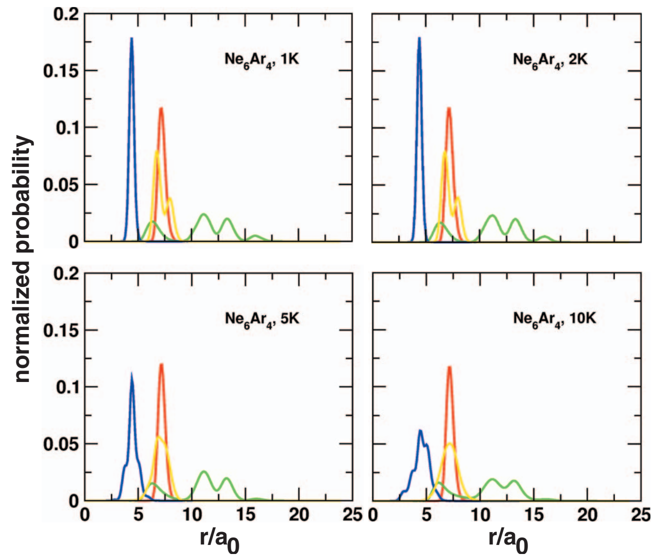

FIG. 2. Distance distribution functions for different atom-atom distances in Ne_6Ar_4 at temperatures of 1, 2, 5, and 10 K. (red: Ar–Ar; green: Ne–Ne; blue: Ar–CoM; yellow: Ne–CoM). The distributions are individually normalized.

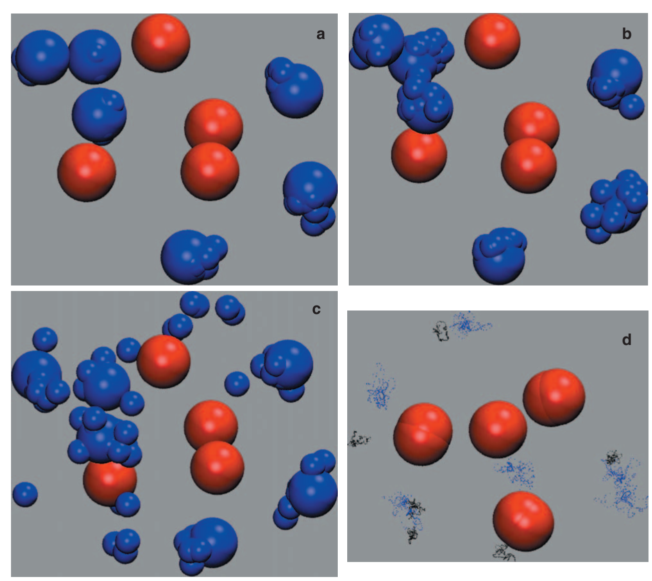

FIG. 3. Snapshots of Ne_6Ar_4 from FPIMC simulations at temperatures $T=1$ K [panel (a)], $T=5$ K [panel (b)], and $T=10$ K [panel (c)]; see also Fig. 2. Red spheres are Ar atoms and blue ones are Ne atoms. In every panel 15 snapshots are superimposed on the Ar atoms which form a tetrahedral arrangement. As temperature increases, the Ne atoms gradually access more of the available conformational space. Panel (d) shows a superposition of one snapshot at $T=1$ and $T=10$ K. Here, the blue (1 K) and black (10 K) traces correspond to the thermal loop of the neon atoms ($k=256$). For higher temperatures the thermal loops become more concentrated, i.e., less quantum.

experimental data. Furthermore, the applicability of FPI-GPA simulations was explored by predicting rotational constants for selected pentamers and for Ne_6Ar_4. The predicted rotational constants for the $n=5$ and $n=10$ clusters should provide valuable information for forthcoming experimental studies of their rotationally resolved spectra. A detailed comparison of total and zero-point corrected ground state energies with rigorous quantum chemical methods [CCSD(T) and MP2 for the smaller and larger clusters, respectively] for trimers and pentamers suggests that many-body effects play a minor role in mixed Ne/Ar clusters.

The influence of many-body effects, in particular, in rare gas systems, has attracted considerable attention over the past few years.[4,5,18] Although their presence has been known for a long time [e.g., the Axilrod–Teller term has been discussed in 1943 (Ref. 19)], explicitly calculating them is computationally very demanding and has only become possible in the past few years.[18,20,21] Recent work has investigated the effect of three-body interactions on melting points and specific heats for argon clusters.[4,5] It was found that the maximum of the heat capacity for Ar_{147} shifts down from 50 to 46 K if three-body interactions are taken into account. This amounts to an effect of $\approx 10\%$. Compared to this, the change in rotational constants with and without three-body interactions in calculating rotational constants for mixed NeAr trimers is much smaller, namely, between 1 and 13 MHz (less than 0.5%) for $^{20}Ne_2{}^{40}Ar$.[3] Thus, it appears that different observables depend on the presence of three-body interactions in distinct manners. In particular, energy-related quantities (such as the bulk energy or the heat capacity $\partial U/\partial T$) may be more sensitive to many-body interactions than structure-related properties, such as rotational constants. This is also found in the present work. Figure 1 compares energy differences from model potentials and CCSD(T)/aug-cc-pvqz calculations for Ne_2Ar. Given that CCSD(T) calculations with complete basis set extrapolation for the Ar_2 pair potential gives virtually indistinguishable results from the fitted potentials,[22] the origin of the different total energies may be in the three-body interactions. On the other hand, the effect of three-body interactions does not seem to affect rotational constants, as is evidenced by previous work[3] and the results in Tables I and II. Similar differences have been found in $Ne_2-HN_2^+$ where three-body contributions were found to be on the order of 65 cm^{-1}, which is consistent with the expectation that in charged systems, the effect of three-body interaction should be larger than in neutral systems.[23]

Finally, it is also of interest to briefly consider alternative means to include nuclear quantum effects in many-body systems. One possibility uses quasiclassical potentials, which are defined as $V_{qc}=V(r)+(\hbar^2/24mk_BT)\Delta V(r)$, where the second term is the Laplacian of the potential energy function.[4,24] Including quantum effects in this way decreases the heat capacity of Ne_{256} clusters from 27 to 26 K.[4] Comparing rigorous quantum finite-temperature simulations and classical simulations with quasiclassical potentials for the present systems will be interesting also because the classical simulations are far less time consuming than FPI-GPA calculations. The present work provides the necessary basis for a meaningful comparison as it establishes the accuracy one can expect for a given intermolecular potential.

ACKNOWLEDGMENTS

The authors acknowledge financial support from the Swiss National Science Foundation through Grant No. 200021-117810 (to M.M.) and the National Science Foundation through Award No. CHE-0095953 (to J.D.D.). M.M. thanks the Chemistry Department of Brown University for generous hospitality during which part of this work has been carried out.

[1] Y. Xu and W. Jäger, J. Chem. Phys. **107**, 4788 (1997).
[2] Y. J. Xu, J. Van Wjingaarden, and W. Jäger, Int. Rev. Phys. Chem. **24**, 301 (2005).
[3] A. Ernesti and J. M. Hutson, J. Chem. Phys. **103**, 3386 (1995).
[4] E. Pahl, F. Calvo, L. Koci, and P. Schwerdtfeger, Angew. Chem., Int. Ed. **47**, 8207 (2008).
[5] E. Pahl, F. Calvo, and P. Schwerdtfeger, Int. J. Quantum Chem. **109**, 1812 (2009).
[6] R. A. Aziz and M. J. Slaman, Chem. Phys. **130**, 187 (1989).
[7] R. A. Aziz, J. Chem. Phys. **99**, 4518 (1993).
[8] F. Y. Naumkin and D. J. Wales, Mol. Phys. **96**, 1295 (1999).
[9] D. A. Barrow and R. A. Aziz, J. Chem. Phys. **89**, 6189 (1988).
[10] J. D. Doll, R. D. Coalson, and D. L. Freeman, Phys. Rev. Lett. **55**, 1 (1985).
[11] M. Eleftheriou, J. D. Doll, E. Curotto, and D. L. Freeman, J. Chem. Phys. **110**, 6657 (1999).
[12] A. Ernesti and J. M. Hutson, Chem. Phys. Lett. **222**, 257 (1994).
[13] R. J. Le Roy, University of Waterloo Chemical Physics Report No. cp-330, 1992.
[14] MOLPRO, a package of *ab initio* programs written by H.-J. Werner, with contributions from R. D. Amos, P. J. Knowles, A. Bernhardsson *et al.*, version 2000.
[15] M. Meuwly and J. D. Doll, Phys. Rev. A **66**, 023202 (2002).
[16] H. Han, Y. Li, X. Zhang, and T. Shi, J. Chem. Phys. **127**, 154104 (2007).
[17] M. J. Frisch, G. W. Trucks, H. B. Schlegel *et al.*, GAUSSIAN 03, Revision B.04, Gaussian Inc., Wallingford, CT, 2004.
[18] A. J. Stone and A. J. Misquitta, Int. Rev. Phys. Chem. **26**, 193 (2007).
[19] B. M. Axilrod and E. Teller, J. Chem. Phys. **11**, 299 (1943).
[20] V. F. Lotrich and K. Szalewicz, J. Chem. Phys. **106**, 9668 (1997).
[21] R. Bukowski and K. Szalewicz, J. Chem. Phys. **114**, 9518 (2001).
[22] R. Podeszwa and K. Szalewicz, Chem. Phys. Lett. **412**, 488 (2005).
[23] M. Meuwly, J. Chem. Phys. **111**, 2633 (1999).
[24] F. Calvo, J. P. K. Doyle, and D. J. Wales, J. Chem. Phys. **114**, 7312 (2001).